Cell, Vol. 83, 743–752, December 1, 1995, Copyright © 1995 by Cell Press

Asymmetrically Distributed PAR-3 Protein Contributes to Cell Polarity and Spindle Alignment in Early C. elegans Embryos

Bijan Etemad-Moghadam, Su Guo, and Kenneth J. Kemphues
Section of Genetics and Development
Cornell University
Ithaca, New York 14853

Summary

The *par-3* gene is required for establishing polarity in early C. elegans embryos. Embryos from *par-3* homozygous mothers show defects in segregation of cytoplasmic determinants and in positioning of the early cleavage spindles. We report here that the PAR-3 protein is asymmetrically distributed at the periphery of the zygote and asymmetrically dividing blastomeres of the germline lineage. The PAR-3 distribution is roughly the reciprocal of PAR-1, another protein required for establishing embryonic polarity in C. elegans. Analysis of the distribution of PAR-3 and PAR-1 in other *par* mutants reveals that *par-2* activity is required for proper localization of PAR-3 and that PAR-3 is required for proper localization of PAR-1. In addition, the distribution of the PAR-3 protein correlates with differences in cleavage spindle orientation and suggests a mechanism by which PAR-3 contributes to control of cleavage pattern.

Introduction

Intrinsically asymmetric divisions, in which cell-autonomous fate determinants are distributed unequally to the daughter cells, play an important role in development (reviewed by Horvitz and Herskowitz, 1992). Two coordinated events are required for an intrinsically asymmetric division to occur: the mother cell must have a polar distribution of fate determinants, and the mitotic spindle must align along the axis of polarity so that daughter cells receive different amounts of the determinants (Rhyu and Knoblich, 1995). Mechanisms by which cell polarity arises and reproducible spindle alignments are controlled have been studied in a variety of metazoan embryos (Goodner and Quatrano, 1993; Gueth-Hallonet and Maro, 1992; Holy and Schatten, 1991). Genetic studies in budding yeast have provided a wealth of molecular detail (reviewed by Chant, 1994), but the relationship between asymmetric divisions in yeast and metazoans is not clear.

The nematode Caenorhabditis elegans offers the opportunity to apply a genetic approach to the study of asymmetric cell division in a metazoan system. The embryonic cleavages leading to the formation of the germline appear to be intrinsically asymmetric and exhibit both polarized distribution of cytoplasmic components and reproducibly oriented cell divisions (reviewed by Priess, 1994; Schierenberg and Strome, 1992; Wood and Edgar, 1994). Mutations affecting cell polarity and cleavage spindle orientation have been identified (Kemphues et al., 1988; Mains et al., 1990; Wood et al., 1980).

The asymmetric divisions of the early embryo are summarized in Figure 1A. The germline blastomeres P0, P1, P2, and P3 display an obvious polarity and divide asymmetrically. P granules, cytoplasmic inclusions of unknown function, are a useful marker for polarity (Strome and Wood, 1983). These granules are distributed uniformly throughout the cytoplasm of oocytes and newly fertilized eggs, but become localized to the posterior pole during the first cell cycle. They are partitioned into the P1 cell by the first cleavage. Prior to P1 division, the granules localize to the posterior pole and are partitioned into the P2 cell by the cleavage. The polar localization and unequal partitioning of P granules occur again in P2 and P3. In P4, the definitive germline precursor cell, the granules do not become polar and are distributed equally to the daughter cells.

During these asymmetric divisions, the mitotic spindles are reproducibly aligned along the axis of polarity defined by the P granule distribution. Information about how this alignment is controlled has been obtained by studies of the second cleavage division. A summary of the current view is presented in Figure 1B. In wild type, the AB spindle aligns transverse to the long axis of the embryo, orthogonal to the axis of the previous spindle. This is considered the "default" cleavage pattern and is dictated by the 90° migration of the duplicated centrosomes along the nuclear envelope (Strome, 1993). In the germline cell P1, the spindle aligns along the long axis. The centrosome migration takes place just as in AB, but an additional 90° rotation of the centrosome–nuclear complex realigns the spindle along the anterior–posterior (AP) axis (Hyman and White, 1987). The rotation of the centrosome–nuclear complex appears to be driven by an interaction of the microtubules of the asters with a site on the anterior cortex of the P1 cell (Hyman, 1989; Hyman and White, 1987). The nature of this interaction is unclear, but results of cytochalasin treatments suggest a role for microfilaments (Hyman and White, 1987). Consistent with this possiblity, actin and actin-capping protein accumulate at a site on the anterior cortex of P1 at the appropriate time in the cell cycle to be mediating the rotation (Waddle et al., 1994).

Maternal effect mutations in five *par* genes result in disruption of AP polarity in the early embryo and also affect spindle position and orientation (Cheng et al., 1995; Kemphues, 1989; Kemphues et al., 1988; Morton et al., 1992). Several aspects of polarity are affected. The normally unequal first cleavage is equal, P granules are mislocalized, and differences in cell division times between the blastomeres are lost. In addition, SKN-1, a transcriptional regulator that is asymmetrically distributed in cells of the wild-type early embryo, is symmetrically distributed in *par-1* embryos (Bowerman et al., 1993). The null mutant phenotypes are not identical among the genes, however. For example, P granules are completely mislocalized in *par-1*

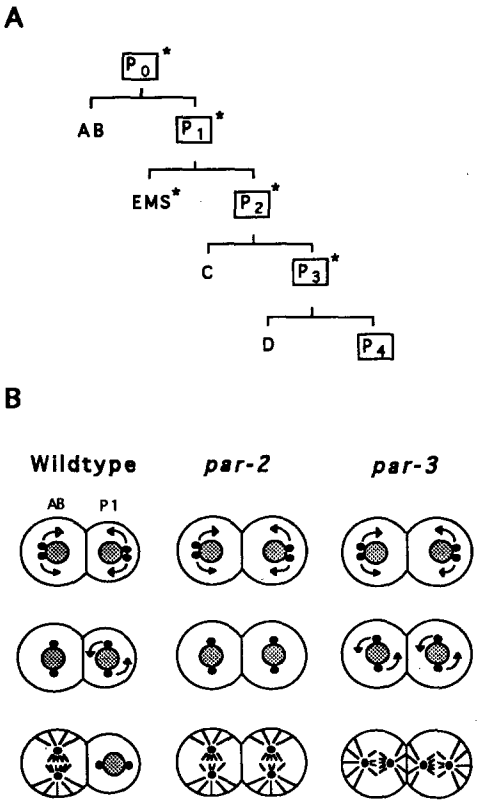

Figure 1. Early Cell Lineage and Cleavage Pattern

(A) Lineage diagram showing the generation of founder cells in the early C. elegans embryo. Boxes indicate blastomeres that contain P granules. Blastomeres undergoing unequal cleavage are indicated by an asterix.

(B) Schematic diagram of spindle orientations in 2-cell embryos from wild-type and homozygous *par-2* and *par-3* mothers. Replicated centrosomes (small closed circles) migrate to opposite sides of the nucleus (stippled circles). Centrosome migration is followed by a 90° rotation of the centrosome–nuclear complex in wild-type P1 and in both blastomeres of *par-3* 2-cell embryos, establishing the plane of the second embryonic division along the AP axis. In *par-2* embryos, no centrosome–nuclear rotation occurs.

and *par-4* mutants, but are partially localized in *par-2* and *par-3* mutants.

Spindle orientation is also affected differently by mutants in the four genes (see Figure 1B). At the second division, for example, in *par-2* and *par-5* mutants, both AB and P1 spindles orient like the wild-type AB spindle, but in *par-3* mutants, both spindles orient like P1 (Cheng et al., 1995; Kemphues, 1989; Kemphues et al., 1988). In *par-1* and *par-4* mutants, most 2-cell embryos show wild-type spindle orientations, but a fraction of the embryos have AB-like spindle orientations in the P1 cell.

The spindle defects observed in *par-2, par-3,* and *par-2 par-3* double mutants indicate that the products of these genes influence spindle orientation at the 2-cell stage by controlling the rotation of the centrosome–nuclear complex that normally occurs only in P1 (Cheng et al., 1995). In particular, the results indicate that *par-3* is required to prevent the rotation of the complex in AB and that *par-2* is required to restrict the *par-3* activity to the AB cell.

The genes *par-1* and *par-2* have been cloned. The *par-2* product is a novel protein with a zinc-binding domain of the so-called RING finger class and an ATP-binding site (Levitan et al., 1994), and *par-1* encodes a putative serine/threonine protein kinase that is localized to the posterior periphery of the zygote and to one pole of asymmetrically dividing cells of the P lineage (Guo and Kemphues, 1995).

In this paper we report that *par-3* encodes a novel protein that is asymmetrically distributed in the zygote and in cells of the P lineage. Like the PAR-1 protein, PAR-3 is found at the periphery of early blastomeres, but its distribution is roughly the reciprocal of PAR-1. Analysis of PAR-1 and PAR-3 protein distributions in other *par* mutants indicates that PAR-3 is partially dependent upon *par-2* for its restriction to the anterior and that PAR-3 asymmetry is necessary for proper PAR-1 localization. In addition, we report that differences in distribution of PAR-3 correlate with differences in spindle orientation.

Results

Identification and Sequencing of the *par-3* Gene

As a first step toward molecular analysis of the *par-3* gene, we mapped *par-3* to the 0.2 MU interval between the markers *daf-4* and *sma-4* on chromosome III. *daf-4* had been previously cloned and placed on the physical map (Estevez et al., 1993). Correlating the physical and genetic maps in this region allowed us to estimate that *par-3* is less than 100 kb to the right of *daf-4*. We tested cosmids

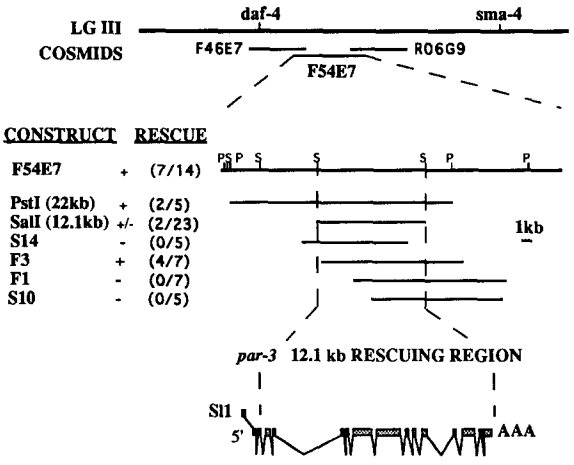

Figure 2. Molecular Cloning of *par-3*

Genetic mapping put *par-3* 0.06 MU to the right of *daf-4*, on chromosome III. The cosmid F54E7 rescued the maternal effect lethality associated with the *par-3* mutation. Horizontal lines under the restriction map show the location of cosmid fragments and genomic phage clones. Constructs were scored as positive for rescue if any progeny were obtained from transgenic worms homozygous for *par-3*. The number of rescuing lines for each cosmid, fragment, or phage are indicated in parentheses. Broken vertical lines indicate the boundaries of the smallest genomic region able to rescue the mutant phenotype. Note that the 12.1 kb fragment does not contain the full message. The *par-3* transcript is *trans*-spliced to the SL1 leader sequence, and the extents of the exons were determined by comparison with the genomic sequence data provided by the C. elegans Genome Project.

to the right of *daf-4* for the ability to rescue the *par-3* phenotype in germline transformation assays (see Experimental Procedures). Figure 2 summarizes the results from germline transformation experiments. Rescue was obtained with the cosmid F54E7, but not with cosmids flanking it on both sides. We subsequently determined the minimum rescuing region by testing gel-isolated restriction fragments of the cosmid F54E7. The smallest genomic region with rescuing ability is a 12.1 kb SalI fragment from F54E7 (Figure 2). To verify that rescue was due to DNA contained in this fragment, we isolated phage from a genomic library using the 12.1 kb fragment as probe and used DNA isolated from these phage in rescue experiments.

To confirm that the rescuing DNA carried the *par-3* gene, we searched for DNA rearrangements associated with *par-3* mutations. We used the smallest rescuing fragment (12.1 kb SalI) as a probe on Southern blots of genomic DNA prepared from heterozygous *par-3* mutant strains. Figures 3A and 3B show blots of DNA from two alleles, *lw30* (a γ-induced allele provided by J. Shaw) and *zu163* (a mutator induced allele provided by C. Mello and J. Priess), that display novel restriction fragments. Both alleles are associated with a shift in a 4.0 kb EcoRI genomic fragment detected by the 12.1 kb probe.

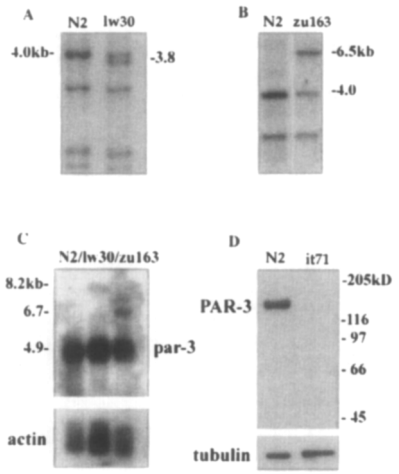

Figure 3. Detection of Allele-Specific Alterations and Immunoblot Analysis of the PAR-3 Protein

(A and B) Southern blots of genomic DNA from wild type (lane N2), *par-3(lw30) lon-1(e185)/qC1* (lane lw30), and *par-3(zu163) lon-1(e185)/qC1* (lane zu163), cut with EcoRI, and probed with the 12.1 kb SalI fragment. In the *lw30* lane, a new 3.8 kb band appears, and the 4.0 kb band is less intense than in the wild-type lane. In the *zu163* lane, a new 6.5 kb band appears. Both the 4.0 and the 6.5 kb bands in the *zu163* lane are about half the intensity of the 4.0 kb band in the N2 lane.

(C) Northern blot of poly(A)$^+$ RNAs isolated from either wild type (lane N2), *par-3(zu163) lon-1(e185)/qC1* (lane zu163), and *par-3(lw30) lon-1(e185)/qC1* (lane lw30) hybridized with a probe made from the *P5A* cDNA. In both *par-3* mutant lanes, a new band of altered mobility appears. An actin probe was used as a loading control.

(D) Western blot of total proteins from extracts of embryos of wild-type (lane N2) and *par-3(it71)* (lane it71) homozygotes probed with anti-PAR-3 antibodies. Monoclonal anti-tubulin antibodies were used as a loading control. The position of migration of molecular markers is shown on the right.

Northern blots of poly(A)-containing RNA showed a single abundant germline-enriched 5.0 kb transcript that hybridizes to the 12.1 kb SalI fragment (data not shown). We later isolated cDNAs from a library (Barstead et al., 1991) using the 12.1 kb fragment as a probe. To determine whether the cDNAs isolated correspond to the *par-3* message, we used the longest one (*P5A*, 4.4 kb) as a probe on Northern blots containing poly(A) RNA from wild-type, *lon-1 par-3(lw30)/qC1*, and *lon-1 par-3(zu163)/qC1* worms. In addition to the 5.0 kb band expected from the wild-type RNA transcribed from the balancer chromosome, each mutant produced a novel band of larger size (Figure 3C). We have not determined the basis for the novel bands. Taken together, the results from germline transformation as well as Southern and Northern blot analyses confirm that the cDNAs we have isolated correspond to *par-3*.

We sequenced the partial cDNA (*P5A*). To obtain DNA sequence corresponding to the remainder of the transcript, we used rapid amplification of cDNA ends and polymerase chain reaction (RACE–PCR) to amplify the missing 5′ end. The combined sequence was submitted to GenBank and is not reproduced here. The 5′ end of the message is *trans*-spliced to the SL1 leader sequence (Bektesh et al., 1988; Krause and Hirsh, 1987), and the message contains an open reading frame that could encode a 1241 amino acid protein with a predicted molecular mass of 138 kDa. No insight into the function of *par-3* was revealed by sequence analysis, as the *par-3* message showed no significant homology to previously cloned genes from the database. Furthermore, an analysis of the predicted structure of the putative *par-3* gene product did not reveal the presence of any conserved domains or motifs. We were able to analyze the genomic sequence from the cosmid F54E7 thanks to the efforts of the C. elegans Genome Sequencing Consortium (Wilson et al., 1994). The transcript is comprised of 15 exons that span 12,494 nt on the chromosome (see Figure 2).

PAR-3 Is Asymmetrically Distributed in the Zygote

We obtained polyclonal antibodies raised against a central portion of the PAR-3 protein by immunizing rabbits with a fragment of PAR-3 fused to glutathione S-transferase (GST) (see Experimental Procedures). Antibodies were affinity purified, and their specificity was examined on Western blots (Figure 3D). A band of the predicted size for the *par-3* gene product (138 kDa) is present in the lane containing wild-type embryo proteins, but is absent from the lane containing proteins from embryos of homozygous *par-3(it71)* hermaphrodites. A faint band of about 125 kDa (barely detectable in Figure 3D) is present in both the wild-type and mutant lanes.

We stained early embryos in gravid worms and examined the pattern of expression of the *par-3* gene product. We found that the distribution of the PAR-3 signal is identical when we use purified antiserum from either of the two immunized rabbits. The staining pattern we describe is not seen with the preimmune serum (data not shown), and embryos from homozygous *par-3(it71)* hermaphrodites show only background staining (Figures 4F and 6C). Fur-

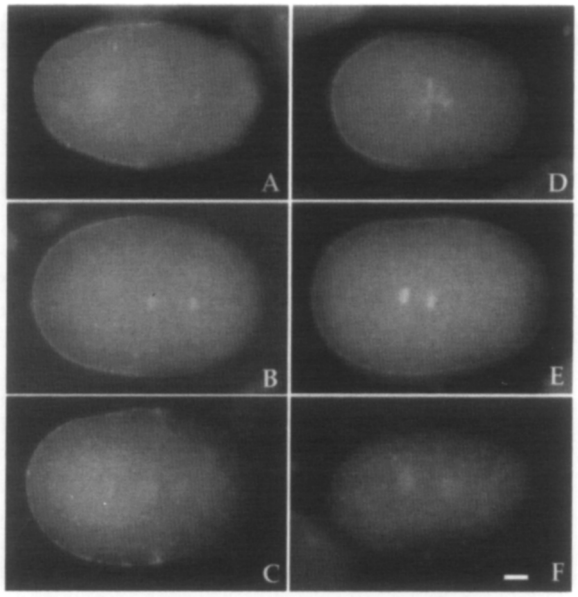

Figure 4. PAR-3 Distribution in 1-Cell Embryos

Double exposure of 1-cell embryos stained for PAR-3 using an FITC-labeled secondary antibody and costained with DAPI. (A–C) Wild-type embryos. (D–F) *par* mutant embryos.

(A) Wild-type 1-cell embryo prior to pronuclear migration. PAR-3 can be seen at the anterior periphery.

(B) Anaphase stage wild type. PAR-3 is at the anterior periphery.

(C) Telophase stage wild type. PAR-3 staining is associated with the cleavage furrow.

(D) A 1-cell *par-1(b274)* embryo. PAR-3 localization is the same as in wild type.

(E) A *par-2(lw32)* zygote. PAR-3 is found at the cell periphery, in a graded distribution with a higher concentration at the anterior, tapering off to a barely detectable amount at the posterior.

(F) No signal can be detected at the periphery of *par-3(it71)* embryos, and the cytoplasmic staining is considerably reduced.

All embryos are oriented with anterior at the left. The scale bar represents 5 μm.

thermore, when purified antibodies are incubated with excess PAR-3 fusion protein prior to the immunostaining assay, no signal can be detected in early embryos (data not shown). We are therefore confident that the staining pattern we describe here represents the distribution of the PAR-3 protein.

No staining is seen in gonads or unfertilized oocytes, but asymmetric peripheral staining develops during the first cell cycle. The PAR-3 protein is first detectable at the cell periphery in fertilized eggs during the meiotic divisions. Of the embryos undergoing first meiotic division, 35% had patchy peripheral staining with no obvious asymmetry (n = 25). The proportion of staining embryos increases during meiosis II; 80% of the embryos stained positively (n = 16). In 10 of the 13 positive embryos, the protein was distributed asymmetrically. The protein was undetectable in the posterior third of the embryo, stained very strongly on the lateral periphery, and stained weakly at the periphery at the extreme anterior pole (data not shown). The other three embryos showed uniform peripheral staining. After meiosis II is completed and as the pronuclei start to decondense, PAR-3 is restricted to the anterior periphery in all cases, extending on average to about 65% of the total length of the embryo (n = 11) (Figure 4A). As pronuclear migration progresses, PAR-3 becomes more concentrated at the anterior pole, and the signal extends, on average, to 54% of embryo length (n = 7). During prophase, metaphase, and early anaphase of the first mitosis, the signal is the strongest and extends to about 48% embryo length (n = 21) (Figure 4B). In late anaphase, the boundary of PAR-3 progresses back toward the posterior pole and extends into the first cleavage furrow near the end of telophase (n = 11) (Figure 4C). In addition to the peripheral staining, at all stages unlocalized PAR-3 appears to be present in the cytoplasm; in *par-3* mutant embryos, the cytoplasmic staining is reduced relative to wild type.

Asymmetric Localization of PAR-3 in the Germline Precursor Cells

PAR-3 is present uniformly at the periphery of AB at all stages of the second cell cycle (n = 25) (Figures 5A, 5B, and 6A). In contrast, we observe cell cycle specificity in the distribution pattern of PAR-3 in the P1 blastomere. In 100% of 2-cell embryos in which nuclei from both AB and P1 are at interphase (n = 10), PAR-3 is either absent from the periphery of P1 or is only present at the extreme anterior of the cell. We believe that the latter is the case for two reasons. First, the intensity of the signal is higher at the boundary of the cells than it is at the outer periphery of AB (Figure 5A), and, second, the PAR-3 protein seems to be pulled into the cleavage furrow during cytokinesis

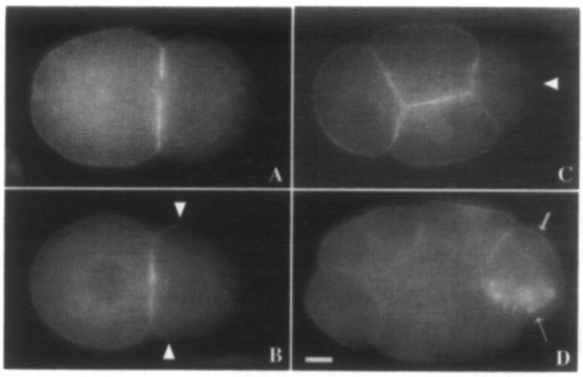

Figure 5. Distribution of PAR-3 in Later Stage Embryos

All embryos were stained with anti-PAR-3 antibodies. (D) was costained with anti–P granule antibodies.

(A) Early 2-cell embryo. PAR-3 is uniformly present at the periphery of AB, and staining is intense at the boundary of AB and P1.

(B) Later 2-cell embryo. PAR-3 is visible at the anterior of P1. The arrowheads show the extent of detectable staining visible in the original micrograph.

(C) Early 4-cell embryo. Somatic blastomeres show staining all around the periphery; intense signal is also seen at the cell boundaries, but no peripheral staining is detected in P2 (arrowhead).

(D) A 7-cell stage embryo. The arrows point to the dividing P2 blastomere. Upon division, P granules (thin arrow) and PAR-3 (thick arrow) are localized on the ventral and dorsal sides of the cell, respectively. PAR-3 is also seen at the periphery of all somatic cells, with stronger staining at the embryonic surface (some blastomeres are out of the plane of focus).

(see Figure 4C). In 93% of embryos in which AB is at prophase (n = 15) and in 100% of later stage 2-cell embryos (n = 93), PAR-3 is present along the anterior 30% of the P1 blastomere (Figure 5B).

At the 3-cell stage, PAR-3 is present all around the periphery of ABa and ABp, and signal is seen at the anteroventral periphery of P1, covering the portion of the cell that will be partitioned into EMS (n = 11) (data not shown). In all 4-cell stage embryos, the three somatic cells show uniform peripheral staining (Figure 5C). In P2, like in P1, the staining is cell cycle dependent. In most interphase P2 cells (24 of 29), staining was restricted to the border of the blastomere bounded by ABp and EMS (Figure 5C); in the remainder of the cells, faint peripheral staining was seen at multiple points on the outer surface as well (data not shown). Some prophase cells (3 of 22) had the staining pattern just described, but most showed a clear asymmetry with strong staining of the dorsal pole of the cell, opposite the P granules (Figure 5D). Later stage P2 cells all showed the polar distribution of PAR-3 (n = 20). The P2 pattern is repeated in P3, with PAR-3 staining only detectable where P3 borders somatic cells early in the cell cycle (n = 10), followed by staining at the pole of the cell opposite the P granules later in the cell cycle (n = 13; data not shown). Because of the peripheral staining in somatic cells, the distribution of PAR-3 in P4 is difficult to score.

In somatic blastomeres, PAR-3 is present all around the cellular periphery, but after the 4-cell stage, the signal becomes asymmetric, with much stronger staining associated with cell membranes that are on the surface of the embryo (Figure 5D). In some embryos, this staining appears as bright circular patches (data not shown). PAR-3 remains detectable until about the 50-cell stage (early gastrulation).

par-2 Is Required to Exclude PAR-3 from the Posterior of the Zygote

To understand better the relationships among the *par* genes, we examined the distribution of PAR-3 protein in *par-1*, *par-2*, and *par-4* embryos. In *par-1(b274)* and *par-4(it57ts)* 1-cell embryos, the distribution of PAR-3 is similar to wild type (n = 38 and n = 20, respectively) (see Figure 4D; data for *par-4* are not shown). In 1-cell *par-2(lw32)* embryos, however, PAR-3 staining is abnormal; staining extends into the posterior of the embryo, although it remains asymmetric. In 67% of the sampled embryos (n = 31), PAR-3 was detectable all around the periphery, but appeared to be distributed in an AP gradient (see Figure 4E). In the remaining embryos, the PAR-3 protein was not detected at the extreme posterior, but in most of the embryos, PAR-3 staining extended more posteriorly than seen in wild type. Thus, *par-1* and *par-4* are not required to localize PAR-3, but *par-2* is required for the restriction of PAR-3 to the anterior.

PAR-3 Distribution Correlates with Spindle Alignment at the 2-Cell Stage

Previous analysis suggested that the gene products of *par-2* and *par-3* act in concert to control the differences in spindle orientation between AB and P1. To understand better the role of PAR-3 in this interaction, we examined the localization pattern of the PAR-3 protein in 2-cell stage *par-2(lw32)* embryos. In 2-cell *par-2* embryos, peripheral PAR-3 staining was found in both blastomeres in most embryos (20 of 22), with the signal slightly stronger around the anterior blastomere (Figure 6B). In 14 of these embryos, the blastomeres were in metaphase or anaphase and could be scored for spindle orientation by examining the DAPI-stained chromosomes. Of these, 12 had *par-2*-like P1 spindles and showed PAR-3 staining around the P1 cell. In two of the embryos, both PAR-3 staining and spindle orientation were like wild type. This is expected because all *par-2* mutations are leaky (Cheng et al., 1995). PAR-3 staining also fails to be restricted in later stages, and no obvious difference is apparent between somatic cells and cells of the P lineage (data not shown).

We also examined PAR-3 distribution and spindle orientation in late stage 2-cell embryos in other mutants that exhibit altered spindle orientations. Most *par-5* embryos and about 20% of *par-1* and *par-4* embryos display transverse spindle orientations in P1 (K. J. K., unpublished data; Kemphues et al., 1988). Of *par-5* 2-cell embryos, 97% examined showed uniform cortical staining for PAR-3 in both AB and P1 cells (n = 36, of which 20 were *par-5(it121)* and 16 were *par-5(it55)*). Of these embryos, ten could be scored for P1 spindle orientation; all had transversely oriented spindles. A wild-type PAR-3 distribution was exhibited by 74% of *par-1* embryos (n = 35) and 88% of *par-4* embryos (n = 24) (data not shown). In the remainder of the 2-cell embryos, the PAR-3 protein was normal in AB, but was distributed over most of the periphery of P1 (*par-1*

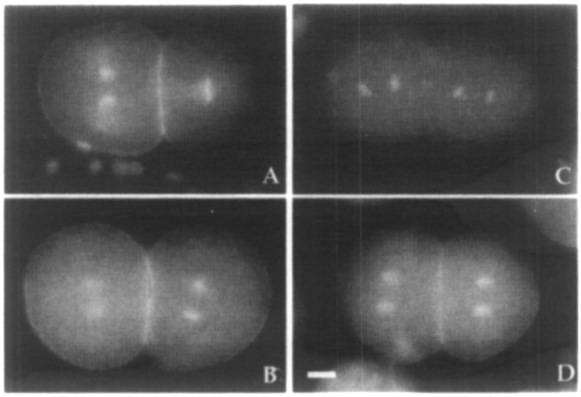

Figure 6. PAR-3 Distribution Correlates with Spindle Orientation

Embryos at 2-cell stage stained for PAR-3 and costained with DAPI.

(A) Wild-type embryo shows PAR-3 uniformly distributed at the periphery of AB and asymmetrically localized to the anterior periphery of P1. The anaphase mitotic figure in AB indicates a transverse spindle orientation; the metaphase figure in P1 indicates a longitudinal one.

(B) *par-2(lw32)* embryo, with peripheral PAR-3 staining and transverse orientation in both blastomeres.

(C) *par-3(it71)* embryo, with no peripheral staining and longitudinal spindle orientation in both blastomeres.

(D) *par-1(b274)* embryo, with extensive peripheral PAR-3 staining and transverse P1 spindle orientation.

The scale bar represents 5 μm.

is shown in Figure 6D; data for *par-4* are not shown). Thus, in embryos with normal distributions of PAR-3, spindle orientation was like wild type, while in embryos with abnormal distribution of PAR-3, the P1 spindle was oriented transversely.

par-3 Is Required for Asymmetric Distribution of PAR-1

The PAR-1 protein is asymmetrically distributed in the zygote and P lineage blastomeres (Guo and Kemphues, 1995) (also Figures 7A and 7C). In fact, comparing the distributions of PAR-1 and PAR-3 throughout embryogenesis reveals that they are roughly reciprocal.

To elucidate a possible interaction between PAR-1 and PAR-3, we stained *par-3* embryos with antibodies raised against PAR-1. In *par-3* 1-cell embryos, the PAR-1 protein is detected around the entire cell periphery, although in reduced amounts compared with wild type (Figure 7B). In about 80% of the *par-3* zygotes examined (n = 30), the distribution of PAR-1 is graded, with slightly more PAR-1 detected at the posterior. This weak polarity appears to diminish as the cell cycle proceeds, and only about half of the *par-3* 2-cell embryos examined (n = 17) showed this weak polarity. In the 2-cell *par-3* embryo, PAR-1 is present not only at the P1 periphery, but also around the periphery of the AB blastomere (Figure 7D). In later stage *par-3* embryos, PAR-1 is detected around the periphery of all blastomeres, instead of being restricted to the P lineage blastomeres (data not shown).

Discussion

Maternal expression of *par-3* is required for the establishment of AP polarity and control of cleavage pattern in early C. elegans embryos. In this paper, we have described the cloning of *par-3* and shown that it encodes a novel protein that is asymmetrically localized to the anterior periphery of the 1-cell embryo. Restriction to the anterior depends upon the activity of the *par-2* gene, but not upon two other *par* genes, *par-1* and *par-4*. The PAR-3 protein is present in both somatic and germline blastomeres but becomes localized asymmetrically only in the germline lineage. In addition, we find that *par-3* is required for proper asymmetric distribution of PAR-1 protein. Finally, we find a correlation between the distribution of PAR-3 and the ability of 2-cell stage blastomeres to undergo the nuclear rotation required to reorient the mitotic spindle.

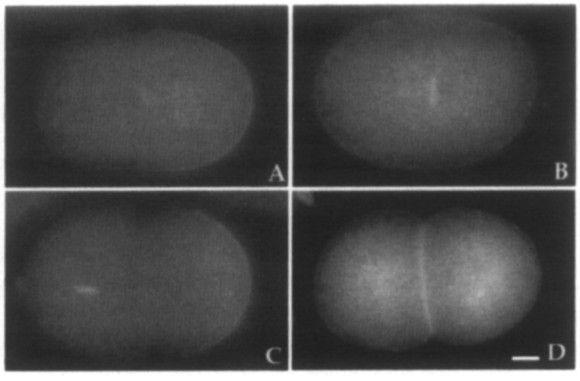

Figure 7. Abnormal Distribution of PAR-1 in *par-3* Embryos

Embryos were stained with anti-PAR-1 antibodies and costained with DAPI.

(A) A 1-cell N2 embryo at metaphase. PAR-1 is present at the posterior periphery.

(B) In 1-cell *par-3(it71)* embryos, PAR-1 is fainter but visible all around the periphery.

(C) A 2-cell wild-type embryo. PAR-1 is localized to the posterior periphery of P1.

(D) A 2-cell *par-3* embryo. The PAR-1 signal is fainter, but visible in both blastomeres. Staining is also intense at the boundary where AB and P1 meet.

The scale bar represents 5 μm.

Establishment of the AP Axis in the Zygote

C. elegans embryos start to display AP polarity during the first cell cycle. P granules become localized to the posterior pole of the zygote (Strome and Wood, 1983), microfilaments concentrate at the anterior (Strome, 1986), and cytoplasm streams along the AP axis (Hird and White, 1993; Nigon et al., 1960). The mitotic spindle is asymmetrically placed, and cleavage produces two daughter cells of unequal size. These daughters exhibit different developmental potential and differential distributions of important regulatory molecules. For example, SKN-1 protein is present at higher concentration in the posterior daughter (Bowerman et al., 1993), and GLP-1 protein is translated only in AB and its daughters (Evans et al., 1994).

We have only a rough understanding of how this polarity is established. Unlike polarity in most other animal models where at least one axis is established during oogenesis, polarity in C. elegans seems to arise de novo after fertilization. The sperm sets the AP axis (B. Goldstein and S. N. Hird, personal communication), and reorganization of cytoplasm during the first cell cycle produces a polarized zygote. The establishment of polarity depends upon microfilaments (Hill and Strome, 1988, 1990) and upon the products of the *par* genes (Kemphues et al., 1988; Kirby et al., 1990). The discovery that PAR-1 and PAR-3 are asymmetrically localized at the cell periphery (Guo and Kemphues, 1995; this paper) suggests that regional differences in the cortical cytoskeleton play an important role in establishing polarity.

PAR-3 has an essential role in the generation of embryonic polarity. In its absence, P granules localize improperly, microfilaments fail to concentrate at the anterior, cytoplasmic streaming is slowed or eliminated, and the first cleavage is equal (Kemphues et al., 1988; Kirby et al., 1990).

Our results suggest that PAR-3 contributes to AP polarity by virtue of its asymmetric distribution at the cell periphery of the zygote. Its appearance at the periphery preceeds (or coincides with) the initiation of cytoplasmic reorganization, starting at the end of meiosis II (Kirby et al., 1990; Nigon et al., 1960), and it becomes distributed asymmetrically before the P granules localize to the posterior, about the middle of pronuclear migration (Rose et al., 1995; Strome and Wood, 1983).

Although the biochemical activity of PAR-3 is unknown,

it appears that one of its roles is to restrict the distribution of PAR-1. PAR-1 is a serine/threonine protein kinase that is localized to the posterior of the zygote and is also required for establishment of polarity (Guo and Kemphues, 1995). Evidence that PAR-3 restricts the distribution of PAR-1 comes from the observation that the distributions of the two proteins are roughly reciprocal and that distribution of PAR-1 is altered in *par-3* embryos, while PAR-3 localization is normal in *par-1* mutant zygotes. It is clear that this is not the only role for PAR-3. As discussed below, PAR-3 also contributes to the regulation of spindle orientation. It is possible, however, that localization of PAR-1 is the major way that PAR-3 contributes to intracellular polarity. Alternatively, PAR-3 could be mediating the localization of multiple cellular components, including PAR-1.

The PAR-2 protein is required to localize PAR-3 in the zygote. In a *par-2* null mutant, PAR-3 distribution extends into the posterior of the zygote, although it retains its asymmetry. Thus, *par-2* plays an important role in localizing PAR-3 but is not the only contributing factor. Combining this result with the PAR-1 results described above, we can construct a simple linear model to describe the relationships among these three genes with respect to their intracellular distribution in the zygote. PAR-2 restricts PAR-3, and PAR-3 restricts PAR-1. Results from studies of the PAR-2 protein, however, indicate that this relationship is more complex. PAR-2 protein is not localized properly in *par-3* mutants (L. Boyd and K. J. K., unpublished data); thus, PAR-2 and PAR-3 proteins are mutually dependent for proper localization.

Role of *par-3* in Maintenance of Germline-Specific Cleavage Pattern

In addition to being localized in the zygote, the PAR-3 protein is asymmetrically localized at the periphery of asymmetrically dividing blastomeres of the P lineage. Thus, PAR-3 may play a role in the germline.

In C. elegans embryos, germline and somatic cells exhibit differences in cytoplasmic composition and cell division patterns. P granules become restricted to cells from the P lineage (Strome and Wood, 1983), and levels of many mRNAs differ between somatic and germline precursor cells (Seydoux and Fire, 1994). P lineage cells all divide along the same axis, while somatic cells divide in an orthogonal pattern (Laufer et al., 1980; Schierenberg, 1987). The *par* genes may act to reestablish polarity at each cell cycle in P1, P2, and P3.

PAR-3 is localized to the side of P1, P2, and P3 that will give rise to the somatic daughter, while PAR-1 is localized to the side of the cell that will give rise to the germline daughter. This distribution is reestablished in each cell cycle. Early in the cell cycle, the peripheral PAR-1 is unrestricted, and PAR-3 is absent or restricted to portions of the periphery bounded by the somatic cells. By late prophase, the proteins have established reciprocal distributions. This observation suggests that these two proteins are part of the machinery necessary for both localization of P granules and unequal oriented cleavages that occur in the germline. Consistent with this, escapers from the maternal effect lethality of weak *par-3* alleles are lacking germline cells (Cheng et al., 1995; Kemphues et al., 1988).

Role of *par-3* in Control of Spindle Alignment

In C. elegans, selection of the cleavage plane plays a major role in the early embryo. The orientation of embryonic divisions determines the position of blastomeres relative to each other, as well as the proper partitioning of cytoplasmic components to daughter cells (Strome, 1993). In early embryos, two different patterns of cleavage are observed. In the descendants of the AB blastomere, equal divisions occur in an orthogonal pattern (Laufer et al., 1980). In the P lineage, the divisions are unequal and are established along the AP axis (Laufer et al., 1980). In our analysis, we find a strong correlation between PAR-3 distribution and cleavage patterns at the 2-cell stage. In wild-type, *par-1*, *par-2*, *par-4*, and *par-5* embryos, PAR-3 is present all around the periphery of cells that fail to undergo nuclear–centrosome rotation. Furthermore, the rotation occurs in all blastomeres where PAR-3 is asymmetrically localized or altogether absent. These results are in agreement with genetic results showing that the *par-3* gene product is not required for the spindle rotation per se, but acts to prevent the rotation in the AB blastomere (Cheng et al., 1995).

Orientation of the mitotic spindle in P1 is thought to be controlled by interactions between cortical components and microtubules emanating from the centrosomes (Hyman, 1989). What cytoskeletal components might PAR-3 interact with to control the division axis? Recent studies in the budding yeast Saccharomyces cerevisiae may provide insights into this question. By disrupting specific cytoskeletal elements using temperature-sensitive mutations, Palmer et al. (1992) demonstrated that spindle position and orientation appear to be mediated by interactions between astral microtubules and the actin cytoskeleton. Recent studies also showed that mutations in dynein heavy chain and an actin-related gene lead to abnormal spindle orientation during mitosis (Eshel et al., 1993; Li et al., 1993; Muhua et al., 1994). Models have recently been proposed in which cytoskeletal proteins become organized in a cell cycle–dependent manner to create a microtubule "capture" site in the newly formed bud (Muhua et al., 1994).

The control of spindle orientation in C. elegans displays many similarities with the yeast model. Previous analysis showed that the centrosome–nuclear rotation in P1 is sensitive to microtubule inhibitors and to laser irradiation of the zone between the centrosome and the anterior cortex of P1 (Hyman, 1989; Hyman and White, 1987). Thus, it appears that the rotation is mediated by microtubules emanating from the centrosomes. The presence of a focus of actin and actin-capping protein at the anterior cortex of P1 during mitosis supports the notion of a temporally and spatially controlled complex of actin and actin-associated proteins necessary for the rotation of the spindle apparatus (Waddle et al., 1994).

Previous genetic analysis and the results reported here suggest that the PAR-3 protein may produce alterations of the cortex that act in preventing the spindle rotation.

This cortical alteration could prevent formation of the anterior cortical site believed to associate with the astral microtubules or could promote interaction of astral microtubules with multiple sites on the cortex to "anchor" the mitotic spindle, preventing rotation. We favor the latter model for two reasons. First, the centrosome–nuclear rotation takes place in the posterior blastomere of both wild-type and *par-3* 2-cell embryos. Thus, the apparent presence of PAR-3 at the anterior periphery of the wild-type P1 blastomere does not prevent the function of the local site. Second, the presence of PAR-3 at the anterior cortex of P1 seems to be necessary for stabilizing the spindle apparatus during or after the rotation (Cheng et al., 1995). If *par-3* embryos are made to undergo second cleavage while under gentle pressure of a coverslip, spindle orientation is more variable than in embryos not subjected to pressure. In wild-type embryos, however, similar treatment does not affect orientation of the P1 spindle. We propose that *par-3* acts to prevent spindle rotation in the AB blastomere by promoting a strong interaction of astral microtubules with cortical components and that this interaction overides the influence of the hypothesized anterior cortical site that drives spindle rotation.

In summary, we propose that asymmetric localization of *par-3* has at least two roles in early embryogenesis. First, PAR-3 restricts the distribution of PAR-1 to the posterior; second, PAR-3 contributes to differences in spindle alignment at the 2-cell stage by promoting stable interaction between astral microtubules and the cell cortex.

Experimental Procedures

Strains and Alleles

Maintenance of C. elegans strains and recombination mapping were carried out using standard techniques (Brenner, 1974). The Bristol strain N2 was used as the standard wild-type strain. The genetic markers and balancer chromosomes used were obtained from the C. elegans Genetic Center, except for the strain *qC1 dpy-19(e1259) glp-1(q339)*, which was provided by J. Austin and J. Kimble. The following mutations were used for genetic and molecular analysis: LGIII, *par-3(it71)*, *par-3(lw30)*, *par-3(zu163)*, *sma-4(e729)*, *daf-4(m63ts)*, *lon-1(e185)*, *unc-32(e189)*, and *par-2(lw32) qC1*; LGV, *par-1(b274)*, *rol-4(sc8)*, *par-4(it57ts)*, *par-5(it121)*, *par-5(it55)*, and *nT1 unc(n754)*.

Three-factor analysis, starting with a *daf-4(m63ts) sma-4(e729)/par-3(it71)* strain, placed *par-3* between *daf-4* and *sma-4*: *daf-4* (10 of 36) *par-3* (26 of 36) *sma-4*. Two-factor analysis placed *sma-4* and *par-3* 0.15 MU apart (9 Sma non-Par of 3023 Sma). Thus, the distance between *daf-4* and *par-3* is approximately 0.06 MU. Map data have been submitted to the C. elegans Genetic Center. We estimated the physical distance of *par-3* relative to *daf-4* by correlating genetic distance from data in the C. elegans database with physical distance obtained from sequence data on chromosome III (Wilson et al., 1994).

Germline Transformation

For transformation rescue, *par-3(it71) unc-32(e189)/qC1* hermaphrodites were injected with a mixture of the DNA to be tested and *rol-6* DNA as a coinjection marker using the procedure of Mello et al. (1991). The mutation *par-3(it71)* causes 100% lethality in embryos from homozygous *par-3* hermaphrodites (Cheng et al., 1995). For each candidate DNA injected, we established a minimum of five *par-3(it71) unc-32(e189)/qC1* lines that transmitted the *rol-6* marker. To test for rescue, we compared the number of progeny produced by 50 each Unc and Rol Unc segregants from each line. To obtain DNA from the rescuing cosmid in λ phage clones, we used the 12.1 kb SalI fragment of F54E7 as a probe to screen a C. elegans genomic phage library (provided by H. Browning).

Cloning and Sequencing

Standard methods were used for Northern and Southern analyses (Sambrook et al., 1989). cDNA clones were isolated from a C. elegans λ cDNA library (Barstead et al., 1991). To sequence the cDNA clone *P5A*, a series of nested deletions were made using exonuclease III and mung bean nuclease (Stratagene). The nested deletions were sequenced using the dideoxy chain terminator method (Sanger et al., 1977). The entire sequence from both strands of the cDNA was obtained. The 5′ end of the transcript was determined using RACE–PCR, according to the protocol of the manufacturer (Clonetech). Sequence analysis was performed using the FASTA program (Pearson and Lipman, 1988) within the Genetics Computer Group package.

Antibody Production and Characterization

A 0.75 kb EcoRI fragment from the smaller *P30A* cDNA was cloned in-frame into the GST bacterial expression vector (Pharmacia); this fragment corresponds to nucleotides 2130–2887 of the transcript. The resulting 54 kDa fusion protein was purified by affinity binding to agarose-immobilized glutathione. Two rabbits were immunized, and the crude antisera were affinity purified over columns containing the PAR-3 fusion protein covalently bound to CNBr-activated 6 Mb Sepharose beads (Pharmacia). Antibodies against the GST portion of the fusion protein were removed by passing the crude serum through a column containing PAR-1–GST fusion protein (Guo and Kemphues, 1995).

To obtain proteins from early embryos for Western blots, we transferred wild-type and *par-3(it71) unc-32(e189)* homozygous worms to 1× PBS on ice. Embryos were then isolated by treating the worms with freshly made bleach solution (1 ml of bleach for 4 ml of 0.66 M KOH) twice for 3 min. The embryos were washed once in M9 solution and resuspended in an equal volume of 2× sample buffer. The samples were boiled for 5 min, and a Pasteur pipette with a flame-closed tip was used to crush the embryos for about 1 min. The samples were boiled for another 3 min and subsequently kept on ice.

Western blots were done by standard procedures (Harlow and Lane, 1988). Samples were run on 7% SDS–polyacrylamide gels, transferred to nitrocellulose, and incubated with either anti-tubulin monoclonal antibodies or anti-PAR-3 antibodies. Visualization used the ECL Western blotting system (Amersham).

Immunofluorescence

For in situ antibody staining with anti-PAR-3 and anti-P granule antibodies, gravid worms were washed in distilled water and transferred in batches of 15 to polylysine slides with 7 μl of PBS and overlaid with 18 mm × 18 mm glass coverslips. Gentle pressure was applied to release the embryos. The slides were placed on dry ice for 15 min. After removal of coverslips, the slides were incubated in methanol at room temperature for 15 min, followed by 5 min in 1× PBS. The samples were blocked with goat serum for 1 hr at room temperature and incubated in diluted antibodies for 2 hr at room temperature. The affinity-purified antibodies were diluted into 1% (w/v) BSA, 10% (v/v) goat serum in PBS. The slides were washed twice for 10 min with PBST (0.5% Tween 20 in PBS) at room temperature, followed by a 10 min wash in PBS. The samples were then incubated for 1 hr at room temperature in secondary antibodies (FITC goat anti-rabbit for PAR-3 and rhodamine goat anti-mouse for P granules). The slides were subsequently washed three times for 10 min in PBST and 10 min in 1× PBS, with a 1/2000 dilution of DAPI included in the second wash. The stained specimens were overlaid with Vectashield (Vector) and a glass coverslip and viewed using fluorescence microscopy. Immunostaining with anti-PAR-1 antibodies was performed according to the method of Guo and Kemphues (1995).

Acknowledgments

Correspondence should be addressed to K. J. K. The authors thank the C. elegans Genetic Center for providing strains, Alan Coulson and John Sulston for providing cosmids, Jocelyn Shaw for *par-3(lw30)*, Jim Priess and Craig Mello for *par-3(zu163)*, Susan Strome for anti-P granule antibodies; and Kathryn Baker and Mona Hassab for technical assistance. We would like to thank Drs. Mariana Wolfner and Michael Goldberg for useful suggestions and critical reading of the manuscript.

This work was supported by National Institute of Health (NIH) grant HD27689. B. E.-M. was supported by NIH predoctoral training grant GM07617.

Received August 9, 1995; revised October 3, 1995.

References

Barstead, R.J., Kleiman, L., and Waterston, R.H. (1991). Cloning sequencing and mapping of an α-actinin gene from the nematode *Caenorhabditis elegans*. Cell Motil. Cytoskel. *20*, 69–78.

Bektesh, S., Van Doren, K., and Hirsh, D. (1988). Presence of the *Caenorhabditis elegans* spliced leader on different mRNAs and in different genera of nematodes. Genes Dev. *2*, 1277–1283.

Bowerman, B., Draper, B.W., Mello, C.C., and Priess, J.R. (1993). The maternal gene *skn-1* encodes a protein that is distributed unequally in early C. elegans embryos. Cell *74*, 443–452.

Brenner, S. (1974). The genetics of *Caenorhabditis elegans*. Genetics *77*, 71–94.

Chant, J. (1994). Cell polarity in yeast. Trends Genet. *10*, 328–333.

Cheng, N.N., Kirby, C.M., and Kemphues, K.J. (1995). Control of cleavage spindle orientation in *C. elegans*: the role of the genes *par-2* and *par-3*. Genetics *139*, 549–559.

Eshel, D., Urrestarazu, L.A., Vissers, S., Jauniaux, J.-C., van Vliet-Reedijk, J.C., Planta, R.J., and Gibbons, I.R. (1993). Cytoplasmic dynein is required for normal nuclear segregation in yeast. Proc. Natl. Acad. Sci. USA *90*, 11172–11176.

Estevez, M., Attisano, L., Wrana, J.L., Albert, P.S., Massague, J., and Riddle, D.L. (1993). The *daf-4* gene encodes a bone morphogenetic protein receptor controlling *C. elegans* dauer larva development. Nature *365*, 644–649.

Evans, T.C., Crittenden, S.L., Kodoyianni, V., and Kimble, J. (1994). Translational control of maternal *glp-1* mRNA establishes an asymmetry in the C. elegans embryo. Cell *77*, 183–194.

Goodner, B., and Quatrano, R.S. (1993). Fucus embryogenesis: a model to study the establishment of polarity. Plant Cell *5*, 1471–1481.

Gueth-Hallonet, C., and Maro, B. (1992). Cell polarity and cell diversification during early mouse embryogenesis. Trends Genet. *8*, 274–279.

Guo, S., and Kemphues, K.J. (1995). *par-1*, a gene required for establishing polarity in C. elegans embryos encodes a putative Ser/Thr kinase that is asymmetrically distributed. Cell *81*, 611–620.

Harlow, E., and Lane, D.P. (1988). Antibodies: A Laboratory Manual (Cold Spring Harbor, New York: Cold Spring Harbor Laboratory Press).

Hill, D.P., and Strome, S. (1988). An analysis of the role of microfilaments in the establishment and maintenance of asymmetry in *Caenorhabditis elegans* zygotes. Dev. Biol. *125*, 75–84.

Hill, D.P., and Strome, S. (1990). Brief cytochalasin-induced disruption of microfilaments during a critical interval in one-cell *C. elegans* embryos alters the partitioning of developmental instructions to the two-cell embryo. Development *108*, 159–172.

Hird, S.N., and White, J.G. (1993). Cortical and cytoplasmic flow polarity in early embryonic cells of *Caenorhabditis elegans*. J. Cell Biol. *121*, 1343–1355.

Holy, J., and Schatten, G. (1991). Differential behavior of centrosomes in unequally dividing blastomeres during fourth cleavage of sea urchin embryos. J. Cell Sci. *98*, 423–431.

Horvitz, H.R., and Herskowitz, I. (1992). Mechanisms of asymmetric cell division: two Bs or not two Bs, that is the question. Cell *68*, 237–255.

Hyman, A.A. (1989). Centrosome movement in the early divisions of *Caenorhabditis elegans*: a cortical site determining centrosome position. J. Cell Biol. *109*, 1185–1194.

Hyman, A.A., and White, J.G. (1987). Determination of cell division axes in the early embryogenesis of *Caenorhabditis elegans*. J. Cell Biol. *105*, 2123–2135.

Kemphues, K.J. (1989). *Caenorhabditis*. In Frontiers in Molecular Biology: Genes and Embryos, D.M. Glover and E.D. Hames, eds. (London: IRL Press).

Kemphues, K.J., Priess, J.R., Morton, D.G., and Cheng, N. (1988). Identification of genes required for cytoplasmic localization in early C. elegans embryos. Cell *52*, 311–320.

Kirby, C., Kusch, M., and Kemphues, K. (1990). Mutations in the *par* genes of *Caenorhabditis elegans* affect cytoplasmic reorganization during the first cell cycle. Dev. Biol. *142*, 203–215.

Krause, M., and Hirsh, D. (1987). A trans-spliced leader sequence on actin mRNA in C. elegans. Cell *49*, 753–761.

Laufer, J.S., Bazzicalupo, P., and Wood, W.B. (1980). Segregation of developmental potential in early embryos of Caenorhabditis elegans. Cell *19*, 569–577.

Levitan, D.J., Boyd, L., Mello, C.C., Kemphues, K.J., and Stinchcomb, D.T. (1994). *par-2*, a gene required for blastomere asymmetry in *Caenorhabditis elegans*, encodes zinc finger and ATP binding motifs. Proc. Natl. Acad. Sci. USA *91*, 6108–6112.

Li, Y.-Y., Yeh, E., Hays, T., and Bloom, K. (1993). Disruption of mitotic spindle orientation in a yeast dynein mutant. Proc. Natl. Acad. Sci. USA *90*, 10096–10100.

Mains, P.E., Kemphues, K.J., Sprunger, S.A., Sulston, I.A., and Wood, W.B. (1990). Mutations affecting the meiotic and mitotic divisions of the early *Caenorhabditis elegans* embryo. Genetics *126*, 593–606.

Mello, C.C., Kramer, J.M., Stinchcomb, D., and Ambros, V. (1991). Efficient gene transfer in *Caenorhabditis elegans*: extrachromosomal maintenance and integration of transforming sequences. EMBO J. *10*, 3959–3970.

Morton, D.G., Roos, J.M., and Kemphues, K.J. (1992). *par-4*, a gene required for cytoplasmic localization and determination of specific cell types in *Caenorhabditis elegans* embryogenesis. Genetics *130*, 771–790.

Muhua, L., Karpova, T.S., and Cooper, J.A. (1994). A yeast actin-related protein homologous to that in vertebrate dynactin complex is important for spindle orientation and nuclear migration. Cell *78*, 669–679.

Nigon, V., Guerrier, P., and Monin, H. (1960). L'Architecture polaire de l'oeuf et movements des constituants cellularies au cour des premières étapes du développment chez quelque nématodes. Bull. Biol. Fr. Belg. *94*, 132–201.

Palmer, R.E., Sullivan, D.S., Huffaker, T., and Koshland, D. (1992). Role of astral microtubules and actin in spindle orientation and migration in the budding yeast, *Saccharomyces cerevisae*. J. Cell Biol. *119*, 583–593.

Pearson, W.R., and Lipman, D.J. (1988). Improved tools for biological sequence analysis. Proc. Natl. Acad. Sci. USA *85*, 2444–2448.

Priess, J.R. (1994). Establishment of initial asymmetry in early *Caenorhabditis elegans* embryos. Curr. Opin. Genet. Dev. *4*, 563–568.

Rhyu, M.S., and Knoblich, J.A. (1995). Spindle orientation and asymmetric cell fate. Cell *82*, 523–526.

Rose, L.S., Lamb, M.L., Hird, S.N., and Kemphues, K.J. (1995). Pseudocleavage is dispensable for polarity and embryogenesis in *C. elegans* embryos. Dev. Biol. *168*, 479–489.

Sambrook, J., Fritsch, E.F., and Maniatis, T. (1989). Molecular Cloning: A Laboratory Manual, Second Edition (Cold Spring Harbor, New York: Cold Spring Harbor Laboratory Press).

Sanger, F., Nicklen, S., and Coulson, A. (1977). DNA sequencing with chain-terminating inhibitors. Proc. Natl. Acad. Sci. USA *74*, 5463–5467.

Schierenberg, E. (1987). Reversal of cellular polarity and early cell–cell interaction in the embryo of *Caenorhabditis elegans*. Dev. Biol. *122*, 452–463.

Schierenberg, E., and Strome, S. (1992). The establishment of embryonic axes and the determination of cell fates in embryos of the nematode *Caenorhabditis elegans*. Semin. Dev. Biol. *3*, 25–33.

Seydoux, G., and Fire, A. (1994). Soma–germline asymmetry in the distributions of embryonic RNAs in *Caenorhabditis elegans*. Development *120*, 2823–2834.

Strome, S. (1986). Fluorescence visualization of the distribution of microfilaments in gonads and early embryos of the nematode *Caenorhabditis elegans*. J. Cell Biol. *103*, 2241–2252.

Strome, S. (1993). Determination of cleavage planes. Cell *72*, 3–6.

Strome, S., and Wood, W.B. (1983). Generation of asymmetry and segregation of germ-line granules in early Caenorhabditis elegans embryos. Cell *35*, 15–25.

Waddle, J.A., Cooper, J.A., and Waterston, R.H. (1994). Transient localized accumulation of actin in *Caenorhabditis elegans* blastomeres with oriented asymmetric divisions. Development *120*, 2317–2328.

Wilson, R., Ainscough, R., Anderson, K., Baynes, C., Berks, M., Bonfield, J., Burton, J., Connell, M., Copsey, T., Cooper, J., Coulson, A., Craxton, M., Dear, S., Du, Z., Durbin, R., Favello, A., Fraser, A., Fulton, L., Gardner, A., Green, P., Hawkins, T., Hillier, L., Jier, M., Johnston, L., Jones, M., Kershaw, J., Kirsten, J., Laisster, N., Latreille, P., Lightning, J., Lloyd, C., Mortimore, B., O'Callaghan, M., Parsons, J., Percy, C., Rifken, L., Roopra, A., Saunders, D., Shownkeen, R., Sims, M., Smaldon, N., Smith, A., Smith, M., Sonnhammer, E., Staden, R., Sulston, J., Thierry-Mieg, J., Thomas, K., Vaudin, M., Vaughan, K., Waterston, R., Watson, A., Weinstock, L., Wilkinson-Sproat, J., and Wohldman, P. (1994). 2.2 Mb of contiguous nucleotide sequence from chromosome III of *C. elegans*. Nature *368*, 32–38.

Wood, W.B., and Edgar, L.G. (1994). Patterning in the *C. elegans* embryo. Trends Genet. *10*, 49–54.

Wood, W.B., Hecht, R., Carr, S., Vanderslice, R., Wolf, N., and Hirsh, D. (1980). Parental effects and phenotypic characterization of mutations that affect early development in *Caenorhadbditis elegans*. Dev. Biol. *74*, 446–469.

GenBank Accession Number

The accession number for the *par-3* sequence is U25032.